Proceedings of the Canadian Society for Mechanical Engineering International Congress
32nd Annual Conference of the Computational Fluid Dynamics Society of Canada
Canadian Society of Rheology Symposium
CSME-CFDSC-CSR 2025
May 25–28, 2025, Montréal, Québec, Canada

Topology optimization of 3D civil structures for buckling resistance: Case of an aluminum footbridge.

Hamadoun Touré[1], Kadiata Ba[1], Sasan Sattarpanah Karganroudi[2]
[1] Applied Science Department, University of Quebec at Chicoutimi, Chicoutimi, Canada
[2]Applied Science Department, University of Quebec at Trois-rivières, Trois-rivières, Canada
*hamadoun.toure1@uqac.ca

Abstract— Topological and geometric optimization is now well developed, yet it remains underutilized in the field of civil structures [1]. Selecting an optimized design that provides reduced weight and high strength while avoiding failures due to high dynamic loads, buckling constraints, or lateral-torsional instability risks is crucial for engineers. Topological and geometric optimization techniques enhance structural performance while reducing weight and design costs [2,3].

This article presents an efficient topology optimization method incorporating key performance criteria for civil structures, including buckling, warping, and dynamic behavior. This method is specifically tailored for designing aluminum footbridges, where traditional design methods are still widely used. The proposed approach optimizes the topology of a 3D structure by minimizing its weight and compliance while ensuring compliance with buckling criteria.

Kreisselmeier-Steinhauser aggregation function is used to combine multiple objectives or constraints into a single objective function, which has shown promising results in prior optimization studies [4]. To address the buckling problem, an eigenvalue problem-solving approach is used to address the buckling problem. The stiffness matrix is assembled using the Cholesky factorization method and incorporates the SIMP (Solid Isotropic Material with Penalization) approach to interpolate density variations within the structure. The results of the static analysis of the optimized longitudinal beams demonstrate a good resistance of $2.65 \times 10^4 Pa$ under a flexion charge of 1.5kN/m^2 with a yield strength of $2.7 \times 10^8 Pa$ and buckling analysis gives a buckling factor of 51.

Keywords- topology optimization; buckling; aluminum; footbridges ; SIMP method.

I. INTRODUCTION

When designing civil structures, it is essential to consider not only the structural strength but also the design and safety standards, such as the CSA S6:19 standard for bridges and footbridges. These standards ensure compliance with strict criteria for durability, safety, and performance under various loading conditions [5]. However, their application often leads to oversized structures. A review of the literature highlights a lack of software tools capable of optimizing the topology of structures based on applied loads while adhering to buckling criteria [6]. Specifically, In the review, I did not find a 3D algorithm that minimizes weight and compliance while respecting the buckling problem in MATLAB using the isotropic material method with the Method of Moving Asymptotes and OC (Optimality Criteria) for updating variables with a scheme.

Among the various optimization methods, the SIMP method (Solid Isotropic Material with Penalization) has been widely used by researchers, particularly through work carried out in MATLAB [7]. This has made it possible to build up a vast database and to make MATLAB particularly suitable as a topological optimization tool, thanks to its ease of use. In addition, compared with other optimizations tools such as Ansys and Abaqus, MATLAB offers greater flexibility for adding other optimization constraints to the main optimizations function, such as buckling constraints, which require advanced calculations and the assembly of large matrices [4,8]. It also enables rapid implementation, particularly for matrix assembly using functions such as fsparse [4], and offers precise control over the choice of filters and the calculation of sensitivities, leading to improved convergence of the optimization solution.

The work of [9] on the development of the MATLAB code top99, aimed at minimizing the compliance of statically loaded structures, was relatively slow. The introduction of new methods based on partial differential equations and black-and-white projection filters by [10] improved results, achieving a 100-fold increase in execution speed for a reference case with 7,500 elements. Advances in filtering and matrix assembly also reduced computation time. Recent progress in the work of [11], increased the execution speed of [10] by factors ranging from 2.55 to 5.5. The 250-line code by [4], which optimizes structures while considering linearized buckling criteria, successfully reduced both the volume and compliance of structures while respecting buckling load factors (BLFs). Topological

Alu Québec – Mitac's

optimization, taking account of buckling stresses, has been extensively studied using the solid isotropic material method with penalization and bidirectional evolutive structural optimization [12]. However, other approaches [13,14] to rapid optimization of 3D topology with buckling constraints, using voxelization, assembly-free deflation and inverse iteration, have further improved optimization performance.

In this work, we present an algorithm developed in MATLAB for the topology optimization of a 3D structure. The algorithm minimizes the structure's weight, maximizes its stiffness, and accounts for buckling criteria. In this work, we address only linear problems. The starting point is the 2D structural optimization algorithm from [4], which incorporates linear buckling criteria in topology optimization. This article is structured as follows. In the first part, we introduce the optimization problem by describing the objective functions, the SIMP method, the physical density calculation method, and the sensitivity analysis. In the second part, the finite element analysis equations for solving the buckling problem are discussed. Finally, we present several numerical examples.

II. Optimization Problem

A. Formulation of the Optimization Problem

Fig. 1 illustrates the proposed methodology. In the first part, the optimization parameters and boundary conditions are defined. The second part involves calculating the physical density of the material. Once the element matrices are calculated, the stiffness and geometric stiffness matrices are determined. Subsequently, the equilibrium equation is solved to determine the eigenvalues and eigenmodes. Finally, the structure is optimized under buckling constraints, and the design variables are updated.

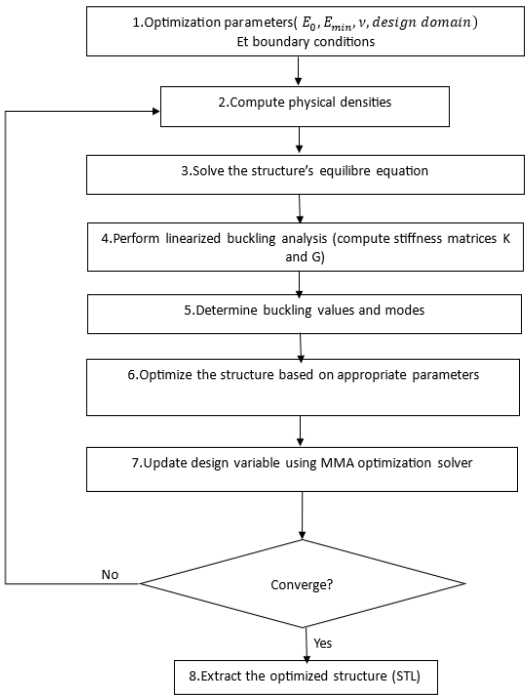

Figure 1: Optimization flowchart

A structured discretized domain Ω_h consisting of mm elements of size Ω_e for a total of n degrees of freedom is considered. The design variable vector $\hat{X} = \{\hat{x}_e\}_{e=1:m\in[0,1]^m}^{m}$ is divided into X_A (active design variables) and X_P (passive design variables).

The optimization problem is solved using a sequential approximation approach. At each redesign step, constraints and objective functions are replaced by their monotonic approximations using the MMA (Method of Moving Asymptotes). Let $\hat{X}$ represent the design variable vector, f $(\hat{X})$ the objective function to be minimized, g_c the compliance constraint, and g_λ the buckling factor constraint. The optimization problem is formulated as follows [4]:

$$\begin{cases} \min\limits_{X\epsilon[0,1]^m} \mathrm{f}(\hat{X}) \\ s.t \quad J_1^{KS}[g_c, g_\lambda](\hat{X}) \le 0 \end{cases} \\ g_c(\hat{X}) = \mathrm{c}(\hat{X})/\bar{c} - 1 \\ g_\lambda(\hat{X}) = 1 - \underline{\lambda} J^{ks}[u_i](\hat{X}) \tag{1}$$

$\mathrm{c}(\hat{X})$ represents the structure's compliance, λ denotes the critical load factor $\bar{c}$ as the maximum allowable compliance, $\underline{\lambda}$ is the prescribed minimum buckling factor, and J^{KS} is the Kreisselmeier-Steinhauser aggregation function.

B. SIMP Method

The Solid Isotropic Material with Penalization (SIMP) method, developed by BendsØe [15], is a topology optimization technique aimed at determining the optimal material distribution within a design domain. It penalizes the density variables using a penalization function f_p

$$ff_{p(x)} \ : [0,1] \longrightarrow [0,1] \tag{2}$$

$$x \longrightarrow x^p$$

Where p is an integer penalization parameter.

The stiffness matrix is constructed by multiplying the material's Young's modulus E_0 by the penalized density:

$$E_i \coloneqq f_p(x_i)E_0 = x_i^p E_0 \tag{3}$$

Where x_i represents the material density in element i, and E_i is Young's modulus of element i. To ensure the design variables evolve within the interval [0,1], the equation becomes:

$$E_i \coloneqq E_{min} + f_p(x_i)(E_0 - E_{min}) \tag{4}$$

Where Emin is Young's modulus of voids($E_{min} = 10^{-8}E_0$).

The SIMP method evaluates the mechanical properties of each element by determining its interpolated Young's modulus. For instance, with penalized SIMP interpolations:

$$E_k(\hat{x}_e) = E_{min} + (E_0 - E_{min})\hat{x}_e{}^{P_k} \tag{5}$$

$$E_G(\hat{x}_e) = (E_0)\hat{x}_e{}^{P_G} \tag{6}$$

Here, P_k and P_G are the penalization factors for compliance and stiffness matrix calculations, respectively.

In general, SIMP modifies the structural properties based on the relative density assigned to each element. These reflect the internal responses of the optimized structure to applied loads.

However, for buckling-constrained problems, continuous relaxation can lead to ill-conditioned stiffness and geometric stiffness matrices involved in the generalized eigenvalue problem [16]. Furthermore, continuous relaxation may introduce unwanted buckling modes, known as parasitic buckling modes. Several model approaches are available to address this issue effectively [4-13].

C. Setup Sensibility

In topology optimization, the variation in material density in each element can affect the objective function. Sensitivity analysis evaluates this variation to guide the process of material removal or addition. We derive the element matrices with respect to $\hat{x}_e$ as follows:

$$\frac{\partial K^e}{\partial \hat{x}_e} = \frac{\partial E_k(\hat{x}_e)}{\partial \hat{x}_e} K_0^e \tag{7}$$

$$\frac{\partial G^e}{\partial \hat{x}_e} = \frac{\partial E_G(\hat{x}_e)}{\partial \hat{x}_e} G_0^e \tag{8}$$

K^e is the stiffness matrix of element e and G^e is the geometric matrix of element e.

The gradients of compliance and structural volume with respect to $\hat{X}$ are given by:

$$\nabla_{\hat{X}} c(\hat{X}) = -U^T \nabla_{\hat{X}} K U \chi_A \tag{9}$$

$$\nabla_{\hat{X}} V(\hat{X}) = \frac{1}{m} 1_m \chi_A \tag{10}$$

Where U is the displacement vector of nodes, $V(\hat{X})$ volume of the structure and H the filtering matrix.

The sensitivities with respect to the design variables are determined by:

$$\nabla_X c(X) = \nabla_{\hat{X}} \mathcal{H} \odot \left(H^T \nabla_{\hat{X}} c(\hat{X}) \right) \tag{11}$$

$$\nabla_X V(X) = \nabla_{\hat{X}} \mathcal{H} \odot \left(H^T \nabla_{\hat{X}} c(\hat{X}) \right) \tag{12}$$

$$\nabla_{\hat{X}} \mathcal{H} = \beta \frac{1 - \tanh\left(\beta(\bar{X} - \eta)\right)^2}{\tanh(\beta\eta) + \tanh(\beta(1-\eta))} \tag{13}$$

The symbol $\odot$ represents element-wise multiplication.

D. Filtering Schemes:

The Heaviside projection is used to binarize the filtered densities into values of 0 or 1, eliminating intermediate density regions. The control parameters β and η must be carefully calibrated to avoid premature convergence during optimization.

When ft=2, the code uses the Heaviside projection, which ensures a binary solution at the end of the optimization process [1].

$$\hat{X}_A = H(\bar{X}) \tag{14}$$

$$H(\hat{x}_e, \eta, \beta) = \frac{\tanh(\beta\eta) + \tanh\left(\beta(\hat{x}_e - \eta)\right)}{\tanh(\beta\eta) + \tanh(\beta(1-\eta))} \tag{15}$$

Where η is the threshold and β is the sharpness factor.

The classical density filter is used to preserve the global material volume in the structure during optimization. It smooths the design variables by performing a weighted average of the densities of neighboring elements. The goal is to avoid undesirable patterns, such as checkerboard designs. When ft=1, the code uses a classical density filter defined by Bourdin [4-17]:

$$\hat{X} = Hx \tag{16}$$

$$H(\hat{x}_e, r_{min}) = \frac{\sum_{i \in N_e} h_{e,i} x_i}{\sum_{i \in N_e} h_{e,i}} \tag{17}$$

Where :

$$N_e = \{i | dist(\Omega_i, \Omega_e) < r_{min}\} h_{e,i=\max(0, r_{min} - dist(\Omega_i, \Omega_e))}$$

III. Eigenvalue Problem Resolution

A. Solution of the Equilibrium Equation:

The equilibrium equation for a linear system of size n is expressed as:

$$\mathrm{Ku} = \mathrm{f} \tag{18}$$

where the stiffness matrix $\mathrm{K} \in \mathbb{R}^{n \times n}$ is symmetric and positive definite, u and $\mathrm{f} \in \mathbb{R}^n$ are the vectors of nodal degrees of freedom and applied forces, respectively.

We used the direct method, which transforms (18) into an equivalent triangular system that can be solved efficiently. Since the stiffness matrix K is symmetric and positive definite, the first step involves its factorization using Cholesky decomposition [4]

$$\mathrm{K} = \mathrm{LL}^{\mathrm{T}} \tag{19}$$

where $\mathrm{L} \in \mathbb{R}^{n \times n}$ is a lower triangular matrix.

This factorization reduces (20) to two triangular systems:

$$\mathrm{L_y} = \mathrm{f\ et\ L^T u} = \mathrm{y, où\ y} \in \mathbb{R}^n \tag{20}$$

However, it is important to note that, unlike K, the Cholesky matrix L is not sparse. Consequently, the explicit factorization of K requires significant storage space. As this resolution is extremely memory-intensive, an alternative approach involves iterative methods, particularly for solving large-scale systems [12].

B. Resolution of the Buckling Problem

The resolution of the generalized eigenvalue problem associated with buckling is a complex task. This section highlights various methods developed to determine the eigenvalues and eigenvectors. The buckling problem is formulated as follows:

$$(\mathrm{K} + \lambda \mathrm{G})\mathrm{v} = 0 \tag{21}$$

where $\mathrm{K}, \mathrm{G} \in \mathbb{R}^{n \times n}$ are the stiffness matrix and geometric stiffness matrix, respectively, and n is the dimension of the problem.

The problem can be reformulated as:

$$\mathrm{Gv} = \mu \mathrm{Kv, où}\ \mu = -\frac{1}{\lambda} \tag{22}$$

Unlike other studies, the objective of this work is to develop an algorithm to optimize the topology of 3D structures, minimizing their weight and compliance while respecting buckling constraints and reducing execution time.

IV. Results and Discussion

Based on the above, we will optimize a cantilever structure as illustrated in Fig.2. The structure is a rectangular domain discretized into design domain $\Omega_h = 48 \times 24 \times 24$ elements. The volume fraction is $f = 0{,}12$, and the filter radius is $r_{min} = \sqrt{3}$, with a Heaviside projection preserving the volume (ft=1). A distributed load is applied along the nodes on the right side, while the left side is fully fixed.

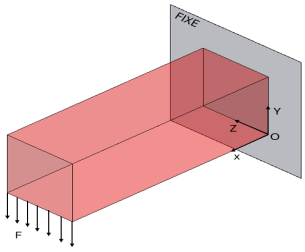

Figure 2: Cantilever with 48 × 24 × 24 elements

Fig.3a shows the optimized structure using the proposed algorithm, while Fig3.b shows the topological optimization using Abaqus software.

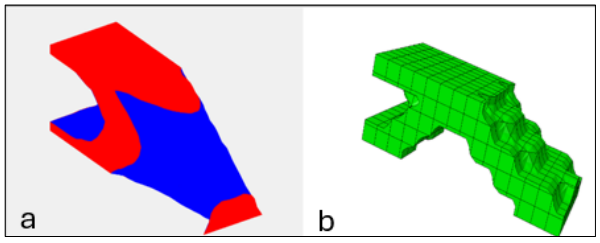

Figure 3: Optimized Cantilever Structures

Both examples share the same boundary conditions and forces are applied to the same elements. However, there is a significant difference in the topology of the two optimized structures. The structure optimized by the proposed algorithm shows a concentration of material in the center, unlike the structure optimized with Abaqus.

A. *Influence of the Filter Type:*

In this section, we address the case of a beam subjected to compression. The design domain of the structure is defined by elements. The left end is fixed, and a pressure F=100 MPa is applied on the right surface, as shown in Fig.4, with ft=1.

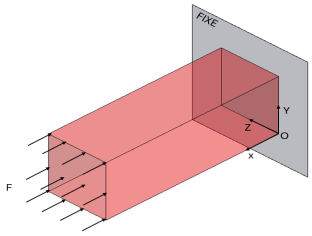

Figure 4: Compression Structure with 60×10×10 Elements

figures 5 show the optimized structure using two different filters. We used the Heaviside projection with ft=2 (Fig.5(b)), which binarizes the optimized element densities and the nearby densities. Additionally, a simple density filter with ft=1 (Fig. 5a) was applied, functioning with a minimal filtering radius. As a result, the two filters produce significantly different topologies. The results of the optimized structures are consistent with the findings of [9].

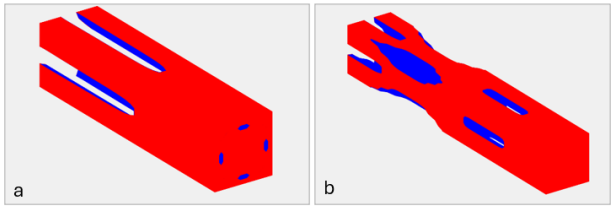

Figure 5: Optimized Compression Structure: a) simple density filter, b) Heaviside projection filter

B. *Creation of Non-Design (Passive) Zones:*

In this section, the objective is to create passive zones (areas where elements remain fixed during optimization). As shown in Fig. 6, the central part is defined as passive, meaning that only the other areas will be modified during the optimization process. This ensures material presence in the center of the structure, unlike the optimization results examples in Fig.5.

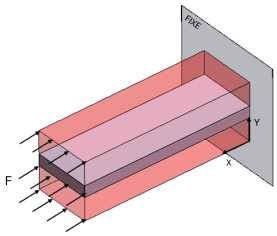

Figure 6:Creation of Passive Zones

After optimization, Fig.7 shows a topology much closer to an I-section. However, as illustrated in View A, there is a concentration of material at one end of the structure, corresponding to the area where the force F is applied. Nonetheless, in View B, an I-shaped profile is visible.

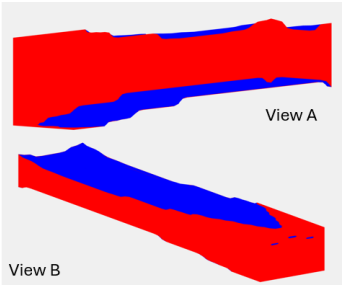

Figure 7: Optimized Structures with Passive Zones

C. *Optimization of Aluminum Footbridge Structures*

The objective of this section is to improve the design of a footbridge structure initially conceived using traditional methods. The footbridge consists of a deck where pedestrians walk, with the loads supported by two longitudinal beams. Crossbeams provide support to the longitudinal beams to prevent lateral buckling, and the entire structure is supported by columns, as shown in the Fig 8. The material is Al6061, young's module E_0=68.9E3MPa and poison's radio $\upsilon = 0.33$

In this work, we will initially focus on the longitudinal beam, as it directly supports all the loads imposed on the footbridge. The initial geometry of the beam is rectangular and discretized into a design domain $\Omega_h = 523 \times 13 \times 20$ elements(fig.9). The maximum allowable volume fraction is $f = 0{,}6$, and the filter radius is $r_{min} = 1.5$, with a Heaviside projection preserving the volume(ft=1).

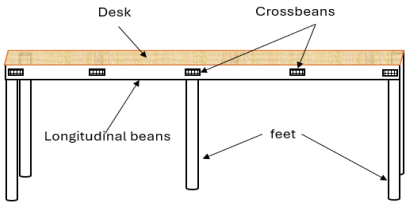

Figure 8: Model of the Footbridge to Optimize

The load supported by the footbridge is evenly divided between the two longitudinal beams. The beam is fixed at both ends, with a uniformly distributed load applied across its upper surface. This load of 3 kN/m2 corresponds to pedestrian loading [16]. Fig. 10 shows the first optimized profile of the longitudinal beam in MATLAB. During the optimization process, the elements subjected to boundary conditions are considered passive.

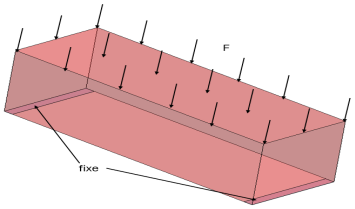

Figure 9: Boundary Conditions Applied to the Longitudinal Beam

As a result, the obtained profile is hollow on the inside while retaining material along the edges subjected to boundary conditions.

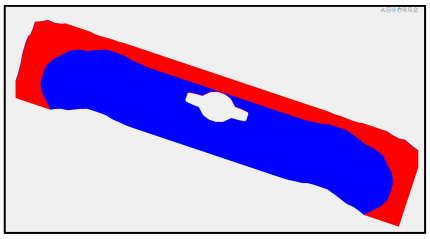

Figure 10: Optimized Longitudinal Beam

For a large filter radius(rmin=3) in fig.11b and (rmin=4) in fig.11a, the filtered density of each element is influenced by a greater number of neighbouring elements, which reduces the geometric precision and leads to a loss of fine details. However, when rmin is smaller (close to 1) in fig.11a, the filtered densities are more refined, and the influence is limited to nearby elements. This allows for more precise details to be preserved in the density distribution.

When the volume fraction is increased to 0.7 in Fig.12a while keeping all other parameters constant, the optimized profile remains like that of Fig.10 from STL. However, when the filter type is changed to a Heaviside projection filter, a significantly different profile is obtained compared to Fig.12a and 12c. Although the topology remains identical, the structure optimized with the Heaviside projection exhibits a much stiffer side, but with instabilities in the regions fixed by the boundary conditions.

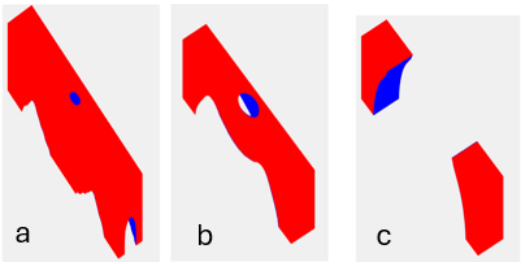

Figure 11: Influence of the filter minimum radius

When the number of elements in the optimized structure is increased (Fig.12a), a hollow begins to appear at the center of the corners fixed by the boundary conditions. However, the lower surface still retains some material.

Additionally, for a volume fraction below 0.55(fig.12d), increased instability is observed, which is also the case for the minimal filter radius. From 1.5 mm onward, instabilities begin to appear in the optimized structure.

As a result, it is observed that the profile of the longitudinal beam tends toward a C-shaped profile. However, the slightly conservative boundary conditions prevent the removal of material at the corners. To address this, the optimized profile can be adjusted to achieve a proper C-shape before scaling it back to its normal dimensions Fig 13.a and validated by element finite analysis.

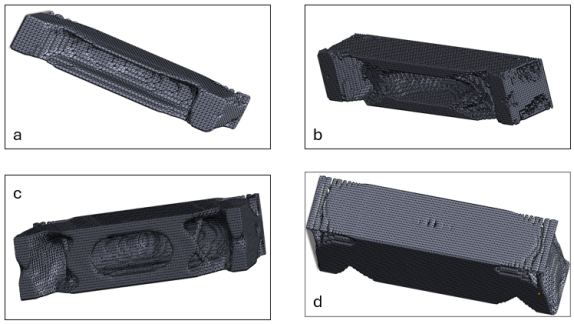

Figure 12: Influence of Optimization Parameters on the Longitudinal Beam(a:Volumefraction 0.7; b: heaviside projection; a:Volumefraction 0.55; d:filter radius 1mm)

A buckling analysis was performed in SolidWorks to verify the resistance of the optimized structure to buckling. First, a static analysis was conducted using the same boundary conditions as in Fig.13b. The optimized structure exhibits a yield strength of $2.710^{8}Pa$, while the maximum recorded stress on the structure is 2.6510^{4}Pa. Second, a buckling analysis Fig.13c was performed. It was observed that the critical part of the structure is located at the center of the piece. However, the buckling factor is significantly greater than 1, with a value of 51, confirming good resistance to buckling. Since the crossbeams do not bear any load but primarily serve to support the longitudinal beams and prevent their lateral buckling, the same optimized profiles can be used for the footbridge design.

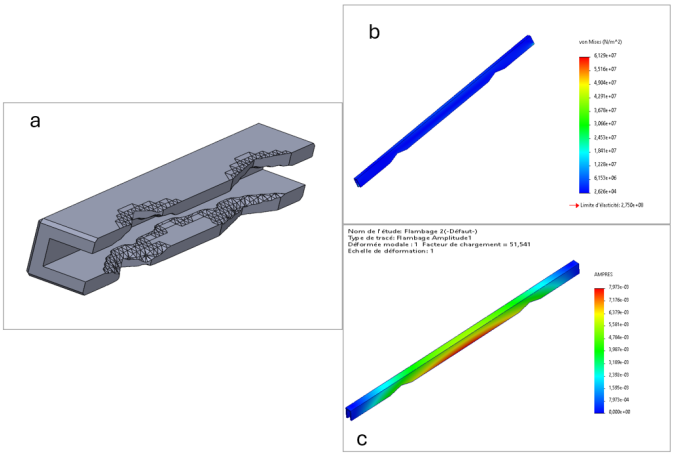

Figure 13: Rectified Optimized Longitudinal Beam in Concept

V. Conclusion

The target of this works to contribute of topology optimization of structures based on applied loads while respecting buckling criteria, thus, an algorithm that optimizes a 3D structure by addressing three primary objectives during the optimization process is proposed:

- Minimizing the weight of the structure,
- Minimizing compliance,
- Respecting buckling constraints.

To address the buckling problem, we used the eigenvalue problem-solving approach, which requires calculating stiffness and geometric stiffness matrices. These matrices were assembled using Cholesky factorization. The Kreisselmeier-Steinhauser (KS) function was employed to aggregate the three objective functions into one, and the SIMP method was used to interpolate density variations within the structure.

We developed optimization examples to validate the performance of the algorithm. The influence of optimization parameters was discussed in this work. It can be concluded that parameters such as the filtering radius, the choice of physical density filtering, and the element size significantly affect the precision of the optimized structure, for large minimal radii rmin the filtered density of each element is influenced by a greater number of neighbours, which reduces geometric precision (loss of fine details). When rmin is smaller (close to 1), the filtered densities are refined, and the influence is limited to nearby elements.

Regarding optimizing the footbridge structure, it is important to develop a strategy to optimize the assembly of the footbridge under buckling constraints. This means optimizing both the longitudinal beams and crossbeams in the same environment to directly determine the optimal number and orientation of the crossbeams during the topology optimization process.

Acknowledgment

Gratitude is extended to AluQuébec and Mitacs for their financial and technical support in the completion of this research project.

References

[1] M.Bruyneel,C.J.Craveur, and P. Cournelen, “Optimisation des structures mécaniques, Méthode numériques et éléments finis.” Dunod, Paris,2014.

[2] G.Parke and N.Hewson, “Ice manual of bridge engeneering”, Institution of civil Engineer, Second edition,2008.

[3] Sétra, “Passerelles piétonnes : Évalution du comportement vibratoire sous l’action des piéto”,2006.

[4] F.Ferrari,O. Sigmund, and K.J. Guest “Topology optimization with linearized buckling in 250 lines of Matlab,” Structural and multidisciplinary optimization Vol. 63, pp.3045–3066, 17 April 2021.

[5] Denis Beaulieu, calcul des charpentes d’aluminium, aluquébec, pp288-506,2023

[6] F.Ferreira and L.Simoes, “Optimum design of a cable-stayed steel footbridge with three-dimensional modelling and control devices”. Elvesier.2019

[7] Y. Zhao,G. Guo, & W. Zuo, “Implémentations MATLAB pour l’optimisation de la topologie 3D géométriquement non linéaire : code de 230 lignes pour la méthode SIMP et code de 280 lignes pour la méthode MMB.” Struct Multidisc Optim 66, 146 (2023).

[8] A. Gupta, R. Chowdhury, A. Chakrabarti, & T. Rabczuk, “ A 55-line code for large-scale parallel topology optimization in 2D and 3D. ” arXiv preprint arXiv:2012.08208,2020

[9] O.Sigmund “A 99 line topology optimization code written in Matlab,” Struc Multidisc Optim pp 120-127,2001

[10] F.Ferrari and O. Sigmund, “A new generation 99 line Matlab code for compliance topology optimization and its extension to 3D.” Structural and multidisciplinary optimization,2020

[11] A.Andreassen, A. Claussen,M. Schevenels,S.B.Lazarov and O.Signmund O, “Efficient topology optimization in Matlab using 88 lines of code,” Struct Multidisc optim, pp1-16,2011

[12] X. Gao and H.Ma, “Topology optimization of continuum structures under buckling constraints,” Computers & Structures ,Vol. 157, September 2015, Pp 142-152.

[13] X.Bian and Z.Fang, “Large-scale buckling-constrained topology optimization based on assembly-free finite element analyse”.Advances in Mechanical Engeneerinf, pp 1-12,2017.

[14] X.Bian, P. Yadav and K.Suresh,K. “Assembly-free buckling analysis for topology optimization.” ASME,pp1-9, 2015

[15] M.P.BensØe And O.Sigmund, “Topology Optimisation: Theory,Methods and Applications.” Sprinder 2024

[16] F.Mitjana,S.Cafieri,F.Bugarin,C.Gogu and F.castanie, “Optimisation of structure under buckling constraints using frame element, Engineering optimization,” 2019.

[17] K.Liu and Tovar, A. “An efficient 3D topology optimization written in Matlab,” Struct Multidisc Optim, pp 1175–1196,2014